

Int

1977,

A Computer Simulation of the Dynamical
Properties of Diatomic Fluids

by

Gerard H. Wegdam,
Physical Chemistry Laboratory,
Nieuwe Prinsengracht 126,
Amsterdam,
The Netherlands,

Gareth J. Evans and Myron Evans,
Department of Chemistry, University College,
Aberystwyth SY 23 1NE.

Short Title

Computer study of diatomics.

Proofs

To Dr. M. W. Evans, at the above address.

5 figures.

Abstract

The recently developed Tildesley/Streett molecular dynamics ¹algorithm for the motion of 256 atom-atom Lennard-Jones potentials is used to study the behaviour of five autocorrelation functions: linear ^{and} angular velocity, orientation, torque and force under the following conditions. (i) Increasing number density (ρ^*) at constant temperature (T^*) and interatomic distance (d^*); (ii) increasing d^* at constant T^* and ρ^* ; (iii) increasing T^* at constant ρ^* and d^* . The following indications appear (i) The mean square torque $\langle Tq^2 \rangle$ and force $\langle F^2 \rangle$ can exhibit maxima or minima as a function of ρ^* or d^* , but over a restricted range, seem linear in T^* at constant ρ^* and d^* . (ii) Autocorrelation functions of high derivatives of the interatomic vector \underline{u} or the angular velocity $\underline{\omega}$ decay generally on the same time scale as the vectors themselves, and become more complicated functions of time. These data do not support an early truncation of the Mori continued fraction with a simple function. (iii) The effect of elongation at constant ρ^* on dynamical properties such as the above is much more pronounced than that of ρ^* at constant d^* indicating that hard-core anisotropy is the important factor in the determination of, for example, ~~renatic~~ ^{nematic} behaviour.

ω omega

Introduction

This paper reports recent work on microscopic fluid dynamics using auto-correlation functions of selected vectors obtained by solving numerically the Newton equation for an assembly of 256 molecules, each of which is represented by a pair of Lennard-Jones atom potentials. The algorithm¹ is a modified version of that which Tildesley and Streett used recently to calculate thermodynamic and other equilibrium properties of computer nitrogen. Atom-atom potential molecular dynamics algorithms^{2,3} were first developed some three years ago, and here we are interested primarily in extending their use to simulate various dynamic properties relevant to spectroscopic studies in such fields as the far infra-red/microwave⁴ or depolarised Rayleigh scattering of light⁵. Both these spectra can be related to the motion of a unit vector \underline{u} in the molecular frame, usually fixed in the dipole moment if this exists. In this paper we observe the behaviour of the 256 molecules under the following conditions.

(i) Increasing the interatomic (interpotential) distance ($d^* = d/\sigma$).

In doing this we effectively change from a pseudospherical molecular shape to a dumbbell, and so measure the effect of increasing geometrical anisotropy on spectral properties (the Fourier transforms of autocorrelation functions) at constant reduced density ρ^* and reduced temperature T^* .

(ii) The recent applications⁶ of memory function formalism⁷ to far infra-red spectra has revealed the need for a detailed study of the behaviour of the ensemble averaged mean square torque $\langle T_q^2 \rangle$ both as a function of ρ^* and d^* . It is also of great interest⁸ to follow the effect on $\langle T_q^2 \rangle$ and $\langle F^2 \rangle$, the mean square force, of increasing temperature at constant ρ^* .

(iii) It is inherent in the projection operator formalism⁹ leading up to the Mori continued fraction approximation¹⁰ to the correlation function of a dynamical variable that at some point a property such as the angular acceleration is deemed to have near $t = 0$ an autocorrelation function approximating to a delta function in comparison with "slow variables" such as the angular velocity or orientation. In this paper we investigate the validity of such a "fast

algorithms

d/σ
↑
sigma

variable" hypothesis by calculating the autocorrelation function of $\ddot{\omega}$ the derivative of the angular acceleration $\dot{\omega}$, and comparing its decay rate with that of \underline{u} , the interatomic vector (normalised to unity), related to $\underline{\omega}$ by $\dot{\underline{u}} = \underline{\omega} \times \underline{u}$.

Computation

The Newton equations are solved by the predictor-corrector method with a time increment of 5×10^{-15} secs. The Lennard-Jones parameters ϵ/k and σ are always those for nitrogen, so we have a "real" molecular system only for $d^* = 0.3292$ - the nitrogen internuclear distance. The thermodynamic stability of the system is judged on criteria such as the constancy of the total pressure, calculated by the virial theorem, and the total internal or configurational energy per molecule. The $\langle Tq^2 \rangle$ and $\langle F^2 \rangle$ terms were calculated with runs of 1600 time steps after rejecting the first unstable few, but were found to be constant essentially after about 200. The stability of the correlation functions can be judged from the comparison of some calculations carried out at 200 and 400 time steps in fig (1). The statistics are adequate since most auto correlation functions are damped to zero in about 50 to 100 steps, as is illustrated in figs (1) to (5). The variation is slight. Using the two-centre potential builds in an anisotropic repulsion core, and the dispersive point is cut off at 3.2σ , so that the whole is representative of geometrical and electrostatic anisotropy. The computations were carried out via the Aberystwyth - U.M.R.C.C. CDC 7600 link in 20 minute segments of real time.

Results and Discussion

Some results are illustrated in figs (1) to (5) in terms of several different autocorrelation functions and as plots of $\langle Tq^2 \rangle$ and $\langle F^2 \rangle$ against reduced number density p^* at a constant temperature and vice-versa. Some features are revealed which can be used to criticize some currently popular models of the fluid state. It is obvious that rotational diffusion is very inadequate, even in its inertia corrected form $\frac{12}{13}$, where the angular momentum auto-correlation function is a single exponential $\frac{13}{12}$, and where the

ω
↑
omega

ϵ/k
↑
epsilon

3.2σ
↑
sigma

[11]

torque auto correlation function is a delta function at the origin. The Mand J diffusion models¹¹ for the motion of the interatomic vector \underline{u} can be derived¹⁴ quite easily ~~using~~ using projector operator formalism¹⁵ wherein the autocorrelation functions of \underline{u} and $\dot{\underline{u}}$ are slowly decaying compared with that of $\ddot{\underline{u}}$. Since the autocorrelation function $\langle \ddot{\underline{u}}(0) \cdot \ddot{\underline{u}}(t) \rangle$ has the units of angular acceleration, it is related to the torque autocorrelation function, which in figs (2) to (5) decays on the same time scale as $\langle \underline{u}(0) \cdot \underline{u}(t) \rangle$. It seems that

$\omega = \omega$
 \rightarrow $\left\{ \begin{array}{l} \langle \underline{w}(0) \cdot \underline{w}(t) \rangle \text{ sometimes decays on a much longer scale (figs (2) to (5)),} \\ \text{but more often it does not. Even the autocorrelation function } \langle \ddot{\underline{w}}(0) \cdot \ddot{\underline{w}}(t) \rangle \\ \text{sometimes takes } \underline{\text{longer}} \text{ to decay than } \langle \underline{u}(0) \cdot \underline{u}(t) \rangle, \text{ and is a much } \underline{\text{more}} \\ \text{complicated function of time than the latter (fig. (1))}. \text{ The Mori continued} \\ \text{fraction representation}^{16} \text{ of } \langle \underline{u}(0) \cdot \underline{u}(t) \rangle \text{ depended partly for its usefulness} \\ \text{on the hope that autocorrelation functions of derivatives of } \underline{u} \text{ might have} \\ \text{had simpler time dependencies than that of } \underline{u} \text{ itself, and could have been} \\ \text{represented empirically. According to our results on nitrogen and rough} \\ \text{dumbbells, both this hope and the fast variable hypothesis are not favoured} \\ \text{by the present computer evaluations. However this does } \underline{\text{not}} \text{ mean that Mori's} \\ \text{equations are conceptually untenable, merely that the successive kernels in} \\ \text{his series are more complicated functions of time than hitherto envisaged. Of} \\ \text{course the memory function series is still an useful way of generating the} \\ \text{whole time dependence of an autocorrelation function knowing only the } \underline{\text{short}} \\ \underline{\text{time}} \text{ behaviour of, say, its second memory function. Below we discuss in more} \\ \text{detail results pertaining to points (i) to (iii) of the introduction.} \\ \underline{T^* = 3.6, d^* = 0.1, p^* = 0.2 \text{ to } 0.8 \text{ (fig. (2))}. \end{array} \right.$

This set of data is intended to simulate the effect of increasing reduced number density on a roughly spherical molecule at constant reduced temperature. Throughout this range the orientational ~~c.c.f.~~^a is inertia dominated, decaying rapidly and exhibiting a secondary maximum similar to that observed by ~~Kneubull~~^{Kneubüke} and Keller¹⁷ for the exceptionally free rotations of HF and HCl in SF₆ solvents. The form of the torque autocorrelation function is very similar but this

has a negative part and tends to oscillate at the higher p^* : having the dimensions of the derivative of angular velocity, the a.c.f. of which decays very slowly compared with the others throughout the whole range of p^* . This means that the overall mean square torque is small in absolute value, since in the limit of vanishing torque the angular velocity a.c.f. would show no decay. It is significant that both $\langle Tq^2 \rangle$ and $\langle F^2 \rangle$ go through a maximum at $p^* = 0.5$, whereas theories of hard collisions and harmonic well oscillations predict a monotonic increase with number density. Recent work on the f. i. c. induced absorption of compressed gaseous ethylene has suggested that $\langle Tq^2 \rangle$ exhibits a turning point with increasing pressure, and similar work on (C_2H_4) and (CS_2) liquids has revealed that $\langle Tq^2 \rangle$ may increase or decrease with temperature at constant p^* .

The force and linear velocity a.c.f.'s have maximum variation through this pressure range. At $p^* = 0.2$ the latter decays very slowly and the former has an extended negative tail. At $p^* = 0.7$ the force a.c.f. oscillates with a long period, and the velocity a.c.f. in turn develops the well-known negative tail, indicative of hydrodynamic coupling, in the limit of very long times, outside our range. The slowly decaying a.c.f.'s at the high p^* are those of angular and linear velocity, although their short time behaviour becomes progressively different. These, together with the fact that there is no apparent shift in the minimum of the orientational a.c.f. shows up the considerable freedom of angular movement and gradual constraint upon translational movement as p^* increases. The oscillatory nature of the force a.c.f. at $p^* = 0.8$ is indicative of the beginnings of "rattling" motion as gradual encaging of a given molecule takes place. The changes in the a.c.f.'s throughout their range are indicative of the nature of the collision rather than any "structuring" in the fluid. At the very highest p^* these are not as forceful as at $p^* = 0.5$, but at $p^* = 0.8$ certain types of encounter are preferred, since there is a narrower spectrum of force and torque. The force a.c.f. is mass dependent and the torque a.c.f. inertia dependent.

$T^* = 3.6, p^* = 0.1, d^* = 0.2 \text{ to } 0.7$ (fig. (3))

The torque increases by an order of magnitude with elongation, and the angular velocity a.c.f. simultaneously decays more quickly. The absolute value of $\langle Tq^2 \rangle$ is small throughout because the molecular number density of the fluid is low. The most interesting aspect of this progression is that the velocity and angular velocity a.c.f.'s get progressively closer together and at $d^* = 0.7$ decay at virtually the same rate, as do those of force and torque ($Tq = d \times F$). The secondary maximum in the orientational a.c.f. disappears progressively with elongation and the decay becomes slower and almost exponential at $d^* = 0.7$. It might be expected that elongation would have a large effect upon rotational movements but it would not be obvious how these would in ~~time~~^{turn} affect the translational aspects of molecular^a motion in this low number density fluid. ~~The computer results show clearly that rotation and translation become strongly correlated as d^* increases.~~ Elongation introduces a degree of ordering into the fluid as shown by the almost exponential decay of the orientational a.c.f. at high d^* . It is apparent from a comparison of this progression with the first studied that elongation has a larger impact than number density in this respect at constant reduced temperature. Here we have the first vague indications of factors important in the formation of a nematic phase - the molecular log jam leading to birefringence.

It is significant that the mean square force becomes progressively smaller with elongation as $\langle Tq^2 \rangle$ ₁₈ increases dramatically, although present analytical theories would be hard pressed to reproduce this accurately. The only one of the five a.c.f.'s to decay more quickly with increasing elongation is that of angular velocity, and this occurs even though the molecular moment of inertia is increasing with d^* , which in the absence of inter-molecular effects, would alone cause the torque, angular velocity and orientation to decay more slowly on the scale of absolute ~~time~~^{ps} (in ~~ps~~). The mass of the molecule is of course unaffected by elongation.

$p^* = 0.643, T^* = 2.3, d^* = 0.1 - 0.7$ (fig. (4))

The mean square torque $\langle Tq^2 \rangle$ behaves as before, but now $\langle F^2 \rangle$ shows a well defined minimum at the nitrogen elongation. At this density there is a pronounced change from gas-like to liquid-like behaviour as the elongation d^* increases at constant T^* . For example, the angular velocity a.c.f. decays slowly at $d^* = 0.1$, but is oscillatory at $d^* = 0.7$, where so are all the other c.f.'s except the orientational, which is nearly an exponential. Hard-core anisotropy must be, in extremis, an important factor in the determination of "structure" in liquids and, in this limit, in the appearance of nematic properties, where the orientational a.c.f. has been observed ^{6a, 21} to be a slowly decaying exponential, and where the memory function, which is $\langle \dot{u}(0) \cdot \dot{u}(t) \rangle$ at $t = 0$, oscillates very rapidly. In an Einstein solid the velocity a.c.f. is a pure cosine, but the nematic phase is characterised by rotational (albeit restricted) and translational freedom, and the forms of the five a.c.f.'s may well be an extreme version of ours at $d^* = 0.7$ for the Lennard-Jones dumbell.

Unlike the longer molecules at $p^* = 0.1$ there is no particular coupling between the rates of decay of velocity and angular velocity, or torque and force, at $p^* = 0.643$, where with $d^* = 0.1$ the velocity a.c.f. decays much more rapidly than the angular velocity, and thereafter at $d^* = 0.7$ both are oscillatory. The linear velocity a.c.f. at $p^* = 0.643$ decays initially much more quickly for the larger molecules, the torque and orientational a.c.f.'s more slowly, but at $d^* = 0.1$, the decay time of the orientational a.c.f.'s at $p^* = 0.643$ and $p^* = 0.1$ are virtually identical, although the linear velocity a.c.f. decays much faster at the higher number density. On the other hand, for $d^* = 0.7$ the velocity a.c.f. at the lower number density is the slower to decay. This elongation at the higher p^* contains translational motion much more effectively, the oscillatory behaviour at $p^* = 0.647, d^* = 0.7$ indicating that the molecules are effectively encaged and "rattling" under torsion. For the longest molecule the decay time of the orientation is much longer at the higher number density.

constrains

The effect of elongation at constant reduced number density on liquid structure is much more pronounced than the effect of p^* at constant elongation, and the built-up hard-core repulsive part of our double Lennard-Jones potential seems dominant in promoting oscillations in some of our a.c.f.'s. Certainly, elongation is much more effective at flattening out the orientational a.c.f.'s, and our data probably explaining why ~~the~~ nematic behaviour seems to be not so much a matter of attractive but rather of repulsive (i.e. molecular ~~shape~~^{shape}) potentials. We will test the effect of quadrupole-quadrupole interaction on forthcoming work.

$$\underline{p^* = 0.6964, d^* = 0.3292, T^* = 1.6 - 2.1 \text{ (fig. (5))}}$$

The mean square torque and force increase linearly with temperature over this admittedly restricted range. This is in accord with harmonic well models, where $\langle Tq^2 \rangle = c kT$, where c is a constant, and hard-core (elastic) models, where $\langle Tq^2 \rangle = (F'/\phi) kT$ where F' is a force coefficient and ϕ ^{phi} is a mean angle of free rotation. In this simulation the reduced number density p^* is kept constant.

$$\underline{T^* = 1.75, d^* = 0.3292, p^* = 0.68 - 0.74}$$

In this range the five a.c.f.'s change very little but $\langle Tq^2 \rangle$ and $\langle F^2 \rangle$ trend upward in value with increasing p^* , although there is an inflexion, or maybe a slight maximum, at $p^* = 0.715$. The elongation of $d^* = 0.3292$ corresponds to *nitrogen*, so our results are for a real molecule at constant reduced temperature. It is interesting to note that $\langle Tq^2 \rangle$ for ethylene, calculated from far infra-red pressure induced adsorption, shows a minimum as pressure decreases at constant temperature ¹⁹. Ethylene is isoelectronic with nitrogen.

It is clear from the varied forms of autocorrelation function displayed here that further experiments (such as scattering of laser radiation, measurement of the depolarisation of fluorescence, infra-red and Raman wings) will be more fruitful when carried out simultaneously on one selected fluid, so that several different aspects of the motion of $\hat{\omega}(t)$ can be discerned. Unfortunately, $\hat{\omega}(t)$ spin-rotation relaxation information on $\langle \hat{\omega}(0) \cdot \hat{\omega}(t) \rangle$

is virtually impossible to obtain at present Larmor frequencies in non-viscous fluids, nor is it probable that any technique will soon directly examine the decay of $\langle \underline{\dot{Q}}(0) \cdot \underline{\dot{Q}}(t) \rangle$. Measurements even of $\langle \underline{u}(0) \cdot \underline{u}(t) \rangle$ at constant p^* and varying T^* are difficult to carry out and very scarce at present.

Those at a constant T^* and varying p^* are much easier.

20

Despite these drawbacks some recent empirical usage of Mori formalism has shown that $\langle Tq^2 \rangle$ does not have a simple experimental dependence on either p^* or T^* , but can go through a maximum or minimum. Figs (2) to (5) reveal such behaviour.

It is clear that a study of $\langle \underline{u}(0) \cdot \underline{u}(t) \rangle$ alone by one experimental technique in isolation disposes of a lot of information by statistical averaging; and in fact experiments on Debye relaxation at frequencies below the far infra-red look at the long-time tail of this autocorrelation function, which is almost always exponential. Such experiments, although difficult and tedious to carry out, thus yield close to the minimum information possible about the trochilics of a typical molecular fluid, even when this happens to be dipolar. Now we are fortunate in having available large computers which, with admittedly rough and ready intermolecular potentials, can be used to yield useful complementary data.

Acknowledgements

G.J.E. and M.W.E. thank the S.R.C. for a studentship and fellowship respectively. M.W.E. thanks the Ramsay Memorial Trust for a fellowship. We are very grateful to Prof. J. S. Rowlinson and Dominic Tild^esley (of Oxford) for invaluable help in the early stages of this work.

References

1. W. B. Streett and D. J. Tildesley, Proc. R. Soc. A., 1976, 348, 485;
S. M. Thompson, D. J. Tildesley and W. B. Streett, Mol. Phys., 1976,
32, 711.
2. P. S. Y. Cheung and J. G. Powles, Mol. Phys., 1975, 30, 921.
3. J. Barojas, D. Levesque and B. Quentrec, Phys. Rev., 1973, 7A, 1092.
4. J. S. Rowlinson and M. Evans, Ann. Rep. Chem. Soc., 1976, ~~in press~~^{5 72A, 5};
M. Evans, in Dielectric and Related Molecular Processes (Chem. Soc.
Specialist Per. Rep.) ed. M. Davies, Vol. 3, 1977, to be published.
5. I. L. Fabelinskii, "Molecular Scattering of Light", Plenum Press, N.Y., 1968.
- 6.a G. J. Evans and M. Evans, J.C.S. Faraday II, 1976, 72, 1169;
b G. J. Davies and M. Evans, J.C.S. Faraday II, 1976, 72, 1194, 1206;
c M. Evans, Spectrochim. Acta, 1976, 32A, 1253, 1259;
d G. J. Davies, G. J. Evans and M. Evans, J.C.S. Faraday II, 1976, 72, 1901.
7. R. Zwanzig, Ann. Rev. Phys. Chem., 1965, 16, 67; B. J. Berne and
G. D. Harp, Adv. Chem. Phys., 1970, 17, 63.
8. G. D. Harp and B. J. Berne, Phys. Rev., 1970, 2A, 975.
9. J. T. Hynes and J. M. Deutch, "Physical Chemistry", ed. H. Eyring,
D. Henderson and W. Jost, Vol. 11B, Chapt. 11, 1975.
10. H. Mori, Prog. Theor. Phys., 1965, 33, 423.
11. W. Steele, Adv. Chem. Phys., 1976, 34, 1.
12. M. Davies, G. W. F. Pardoe, J. E. Chamberlain and H. A. Gebbie, Trans.
Faraday Soc., 1968, 64, 847.
13. G. W. ~~W.~~ Ford, J. T. Lewis and J. McConnell, Proc. R. Irish Acad.,
1976, 76, 117; J. T. Lewis, J. McConnell and B. K. P. Scaife,
Proc. R. Irish Acad., 1976, 76, 43.
14. F. Bliot and E. Constant, Chem. Phys. Letters, 1974, 29, 618;
G. J. Evans, G. Wegdam and M. W. Evans, Chem. Phys. Letters, 1976, 42, 331.
15. D. Kivelson and T. Keyes, J. Chem. Phys., 1972, 52, 4599.
16. B. Quentrec and P. Bezot, Mol. Phys., 1974, 27, 879;
G. Bossis and B. Quentrec, Mol. Phys., 1976, 32, 591.
17. B. Keller and F. Kneubühl, Helvetica Phys. Acta, 1972, 45, 1127.
- 18.a H. N. V. Temperley, J. S. Rowlinson and G. S. Rushbrooke, "Physics of
Simple Liquids", North-Holland, Amsterdam, 1968;
b C. A. Croxton, "Liquid State Physics", Cambridge Univ. Press, 1974;
c A. F. M. Barton "The Dynamic Liquid State", Longman, London, 1974.
19. G. J. Evans and M. Evans, Adv. Mol. Rel. Proc., 1976, ~~in press~~ 9, 1.
20. B. J. Berne and J. A. Montgomery, Mol. Phys., 1976, 32, 363.
21. G. J. Davies and M. Evans, Adv. Mol. Rel. Proc., in press;
G. J. Evans and M. Evans, J.C.S. Faraday II, in press.

Figure (1)

Left to right, top to bottom: normalized autocorrelation functions

(a) Effect of using 400 and 200 time steps on the calculation of

$\langle \underline{u}(\circ) \cdot \underline{u}(t) \rangle$, $d^* = 0.1$, $T^* = 3.6$, $p^* = 0.1$. (1) 400 time steps,
(2) 200 time steps.

(b) as for (a), $d^* = 0.1$, $T^* = 2.32$, $p^* = 0.645$.

(c) Linear velocity autocorrelation function, $d^* = 0.3292 (N_2)$.

(d) as for (a), $d^* = 0.1$, $T^* = 3.6$, $p^* = 0.7$.

(e) $\langle \underline{\omega}(\circ) \cdot \underline{\omega}(t) \rangle$, N_2 , $T^* =$, $p^* =$

(f) " , N_2 , $T^* = 2.2$, $p^* = 0.645$.

(g) " , N_2 , $T^* =$, $p^* =$

(h) " , N_2 , $T^* = 2.0$, $p^* = 0.645$.

Abscissae : time steps.

Figure (2)

Left to right, top to bottom, ($T^* = 3.6$, $d^* = 0.1$):

(a) Plot of $10^3 \langle Tq^2 \rangle$ vs. _____ p^*

(b) Plot of $\langle F^2 \rangle$ vs. _____ p^*

(c) Autocorrelation functions for $p^* = 0.2$: (1) velocity;

(2) orientation; (3) angular velocity; (4) force; (5) torque.

(d) As for (c), $p^* = 0.3$.

(e) " " " $p^* = 0.4$.

(f) " " " $p^* = 0.5$.

(g) " " " $p^* = 0.6$

(h) " " " $p^* = 0.7$.

(i) " " " $p^* = 0.8$.

Ordinates, (a) $10^3 \langle Tq^2 \rangle$; (b) $\langle F^2 \rangle$

Abscissae (a) p^* ; (b) p^* ; (c) - (i) time steps.

Figure 3

Left to right, top to bottom, ($p^* = 0.1, T^* = 3.6$) :

(a) $\langle Tq^2 \rangle$ vs d^* ; (b) $\langle F^2 \rangle$ vs d^* ;

(c) Autocorrelation functions, (1) velocity; (2) orientation;

(3) angular velocity; (4) force; (5) torque; $d^* = 0.1$.

(d) as for (c), $d^* = 0.2$.

(e) as for (c), $d^* = 0.3$.

(f) " " " , $d^* = 0.4$.

(g) " " " , $d^* = 0.5$.

(h) " " " , $d^* = 0.6$.

(i) " " " , $d^* = 0.7$.

Ordinates : (a) $\langle Tq^2 \rangle$; (b) $\langle F^2 \rangle$

Abscissae : (a) d^* ; (b) d^* ; (c)-(i) time steps.

Figure 4

Left to right, top to bottom, ($p^* = 0.643, T^* = 2.3$).

(a) $\langle Tq^2 \rangle$ vs d^* ; (b) $\langle F^2 \rangle$ vs. d^* ;

(c) Autocorrelation functions, (1) velocity, (2) orientation;

(3) angular velocity; (4) force; (5) torque; $d^* = 0.7$.

(d) as for (c), $d^* = 0.5$.

(e) as for (c), $d^* = 0.425$.

(f) as for (c), $d^* = 0.3292$.

(g) as for (c), $d^* = 0.3$.

(h) as for (c), $d^* = 0.2$.

(i) as for (c), $d^* = 0.1$.

Ordinates : (a) $\langle Tq^2 \rangle$; (b) $\langle F^2 \rangle$

Abscissae : (a) d^* ; (b) d^* ; (c)-(i) time steps.

Figure 5

Left to right, top to bottom (for nitrogen)

(a) $\langle Tq^2 \rangle$ vs. T^* at $p^* = 0.6964, d^* = 0.3292$.

(b) $\langle F^2 \rangle$ vs. T^* " " " "

(c) $10 \langle T_q^2 \rangle$ vs. p^* at $T^* = 1.75$, $d^* = 0.3292$.

(d) $\langle F^2 \rangle$ " " " " " " "

(e) Autocorrelation functions, (1) velocity, (2) orientation, (3) angular velocity,

(4) force, (5) torque; $T^* = 1.75$, $p^* = 0.6964$.

(f) as for (e); $T^* = 1.75$; $p^* = 0.68$.

(g) " " " ; $T^* = 1.9$; $p^* = 0.6964$.

(h) " " " ; $T^* = 1.75$; $p^* = 0.74$.

Ordinates : (a) $10 \langle T_q^2 \rangle$; (b) $\langle F^2 \rangle$; (c) $10 \langle T_q^2 \rangle$; (d) $\langle F^2 \rangle$

Abscissae : (a) T^* ; (b) T^* ; (c) p^* ; (d) p^* (e) - (h) time steps.

Fig (1)

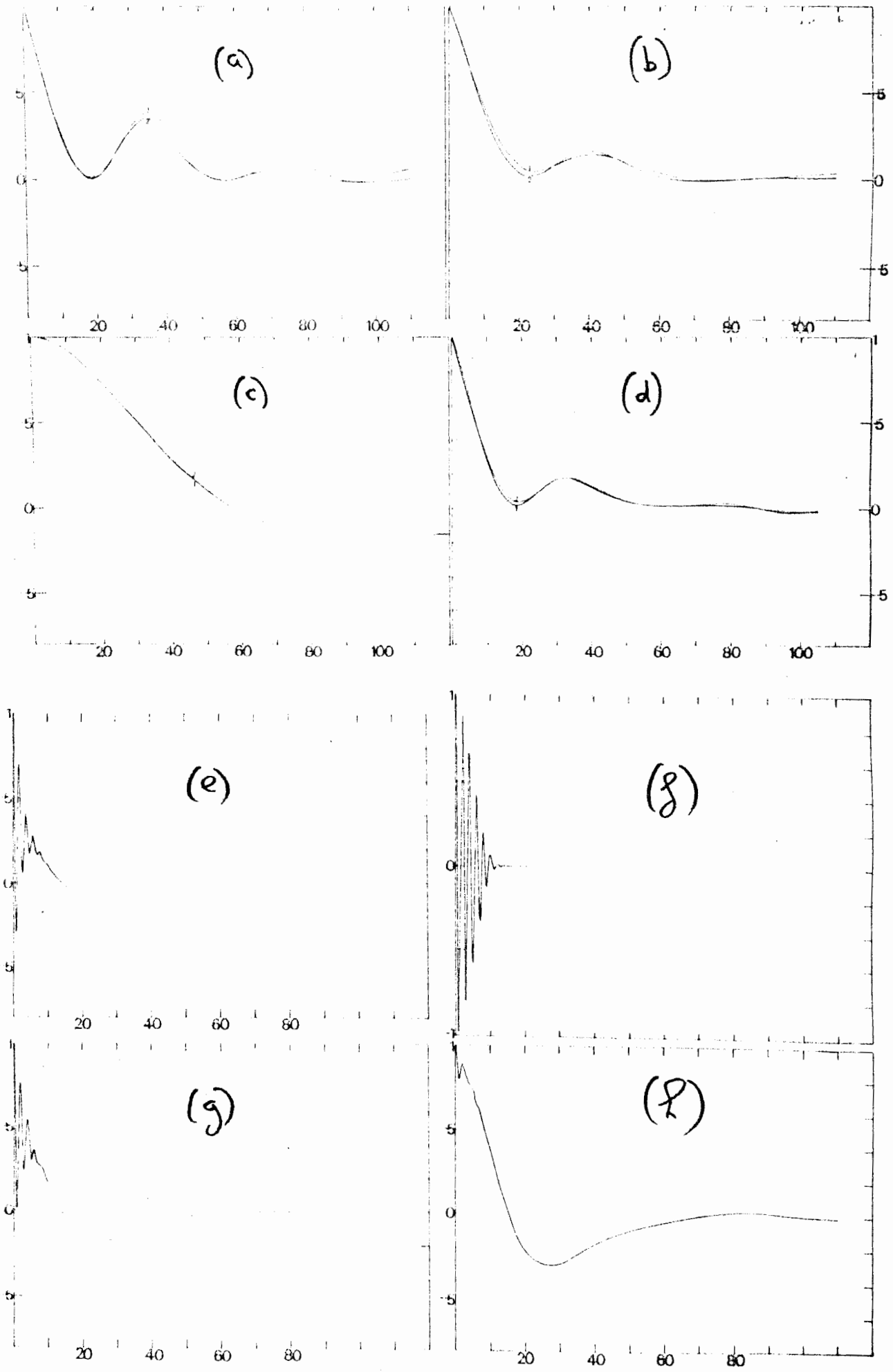


Fig (2)

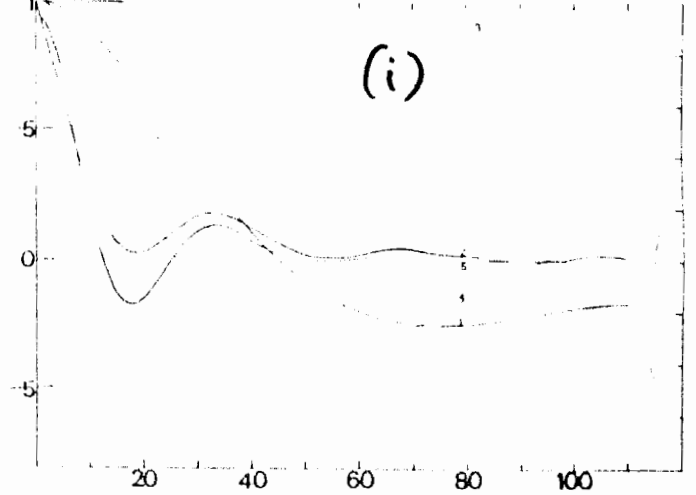
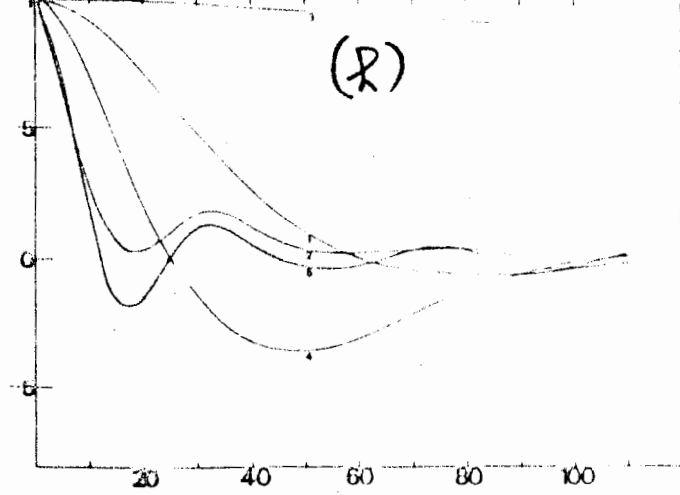
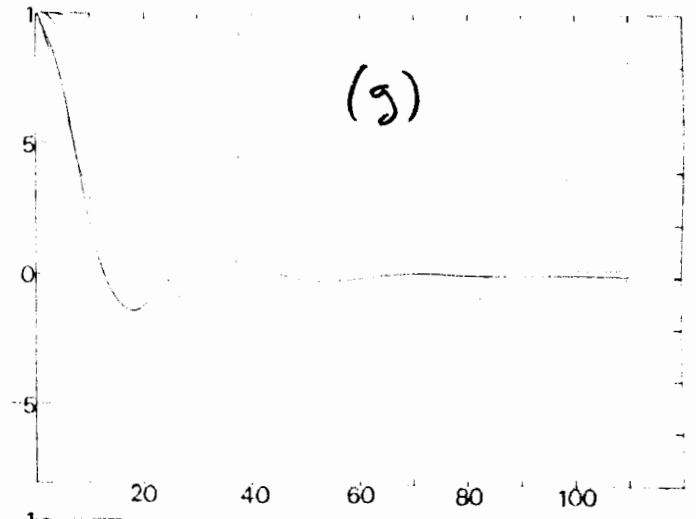
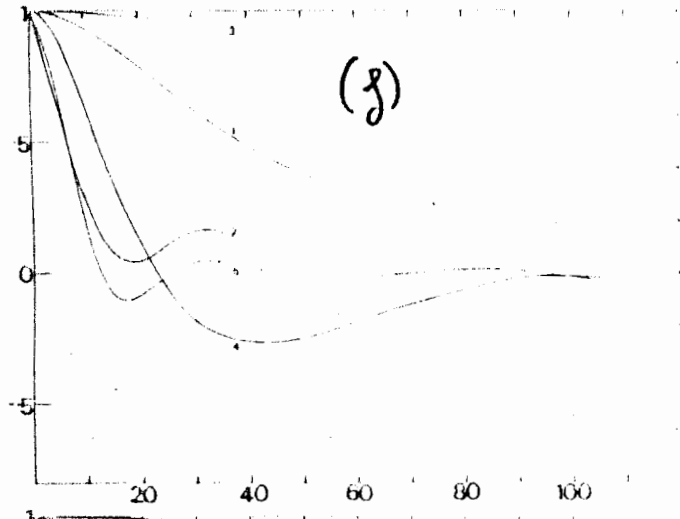
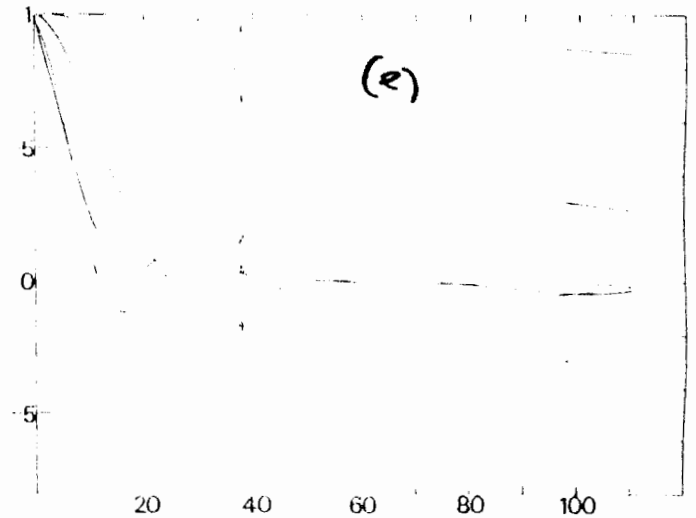
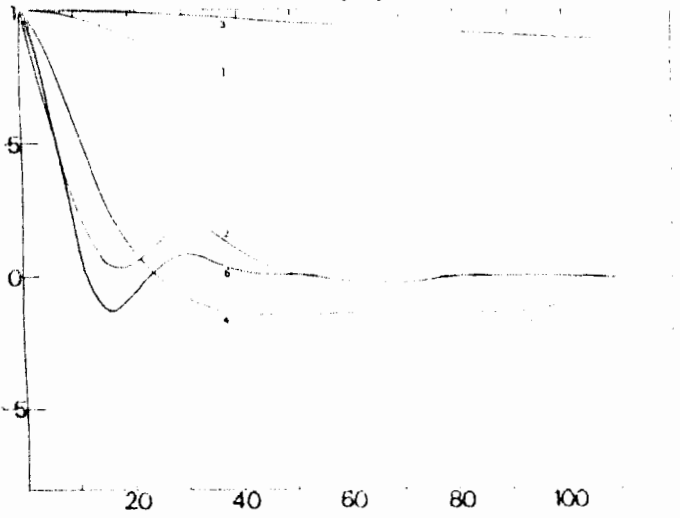
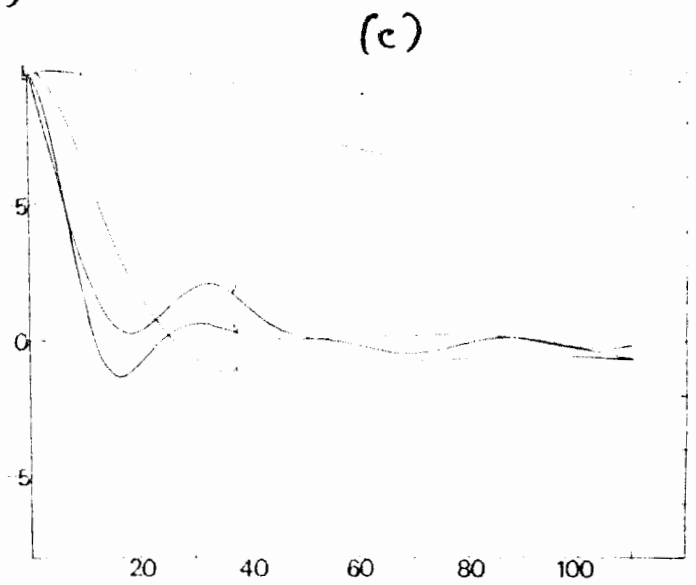
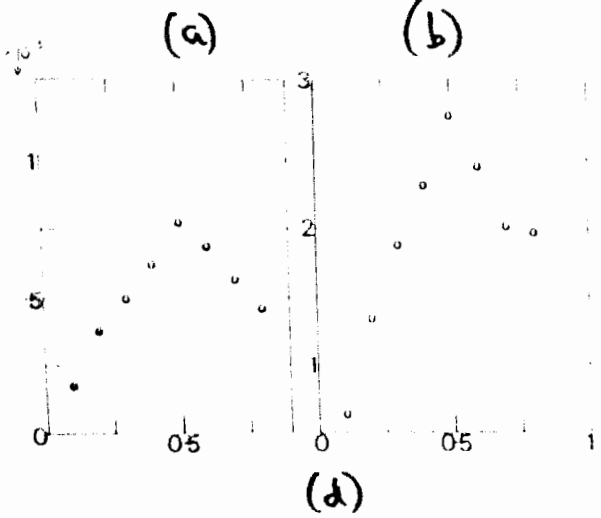


Fig 3

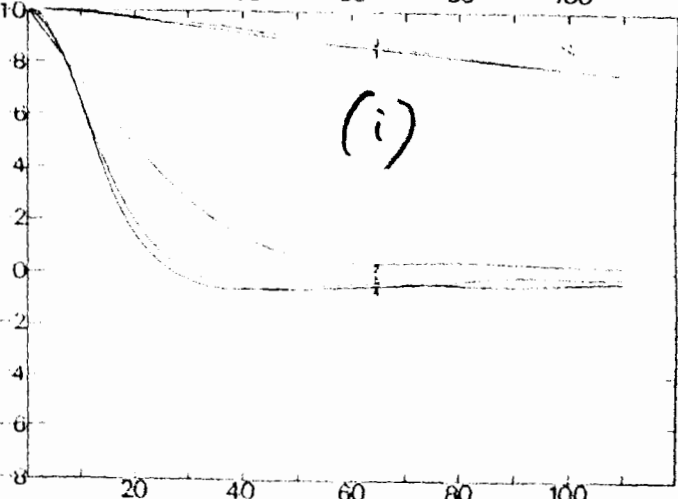
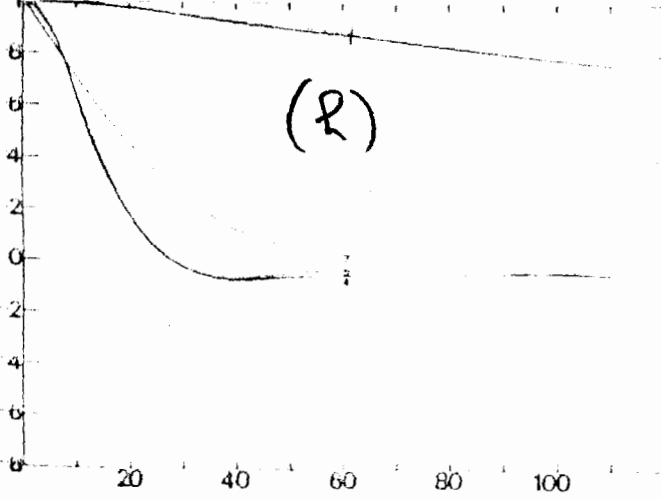
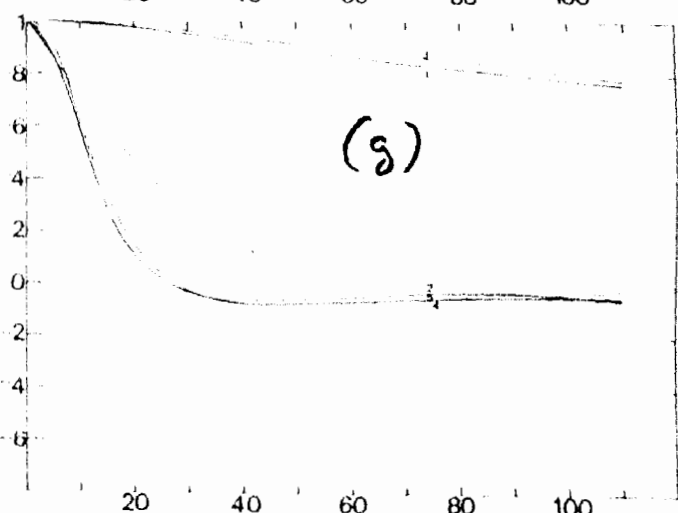
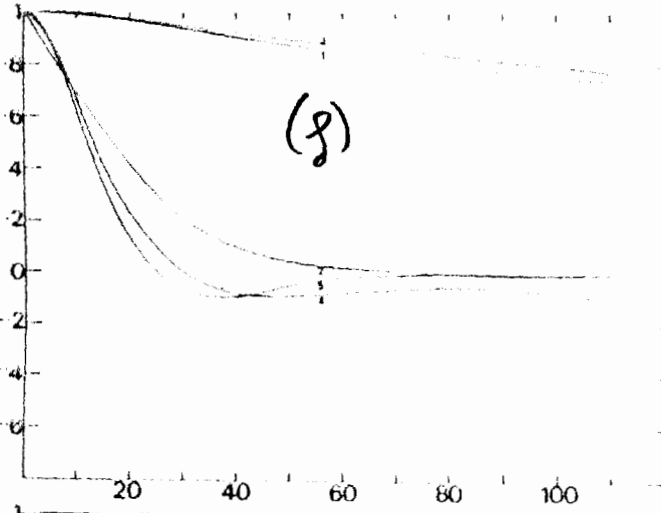
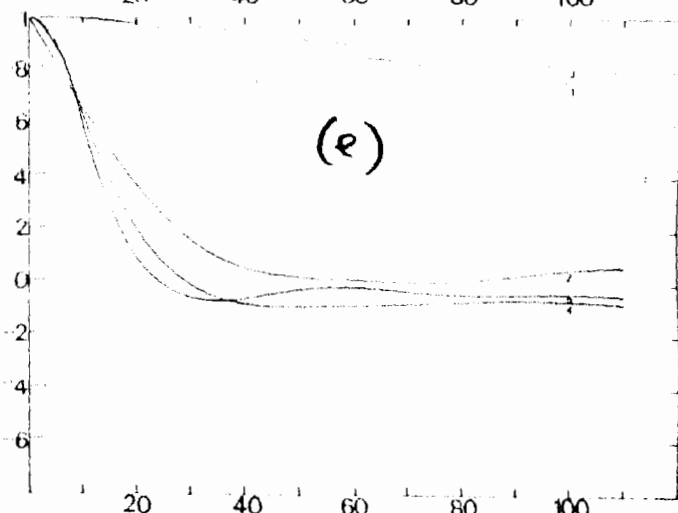
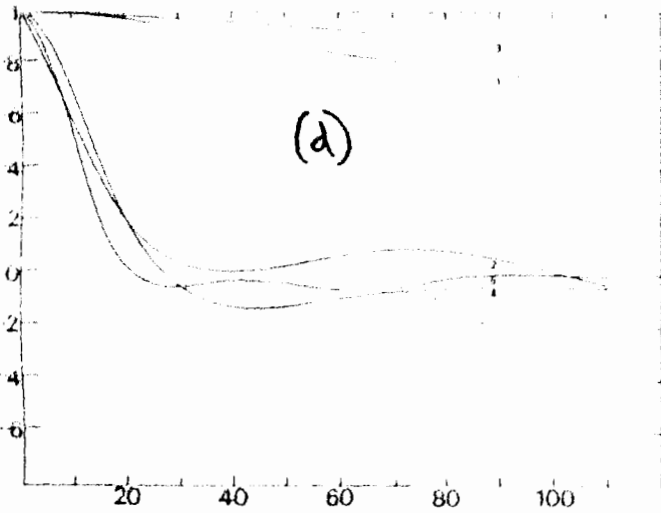
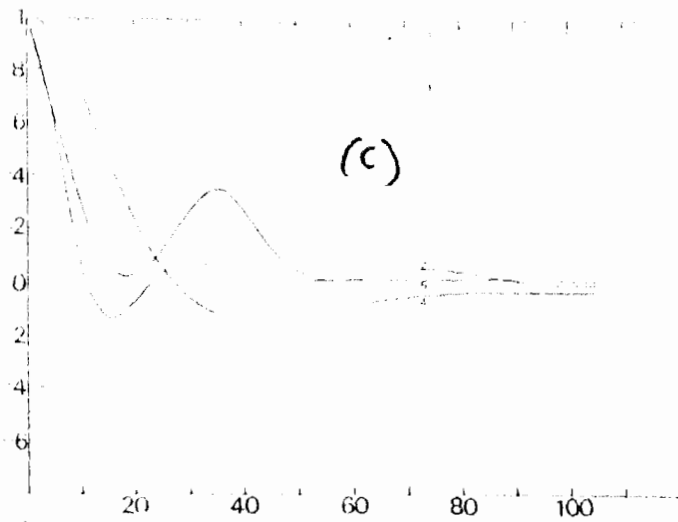
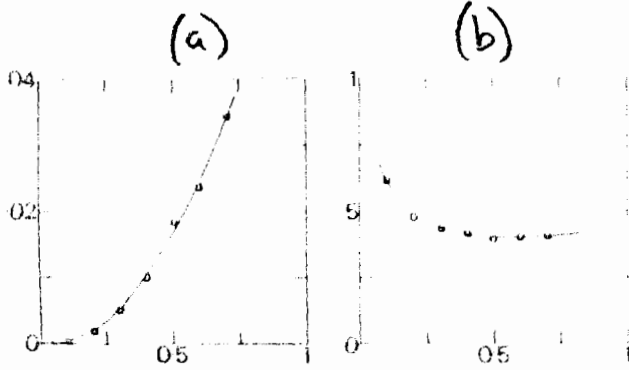


Fig (4)

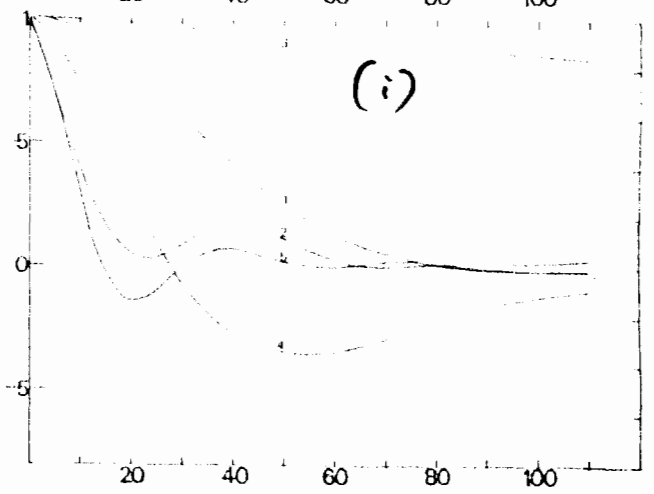
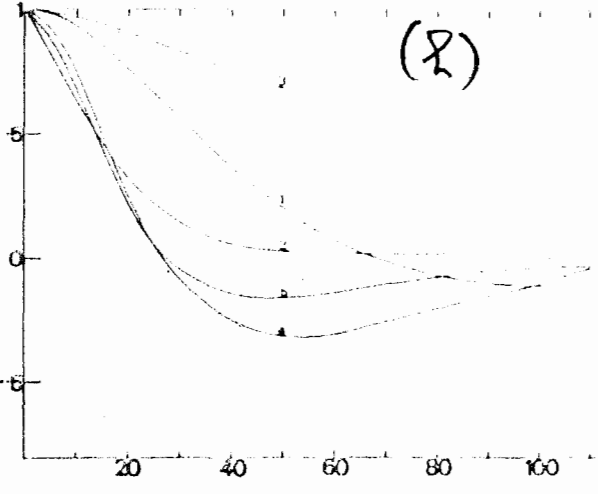
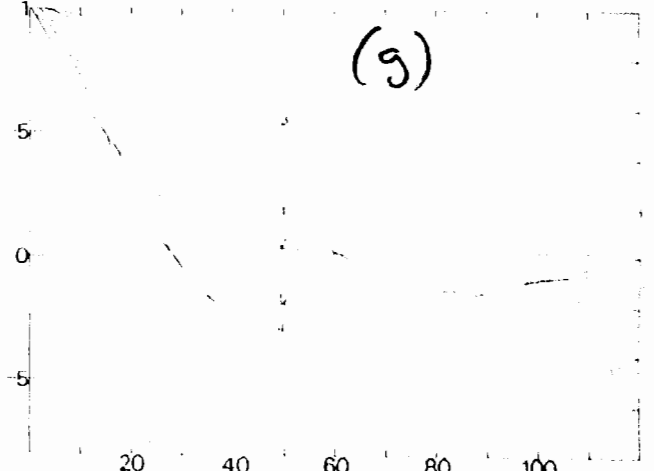
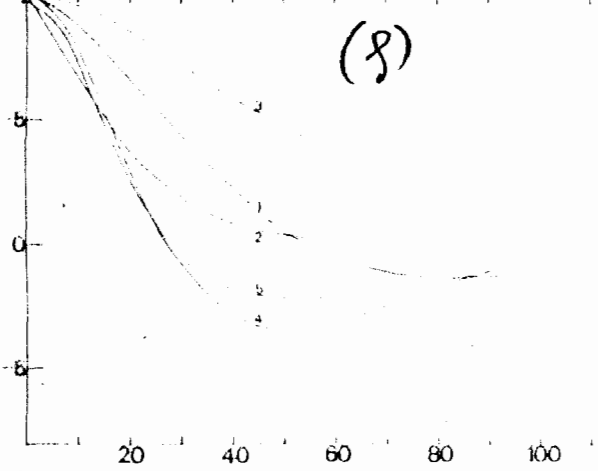
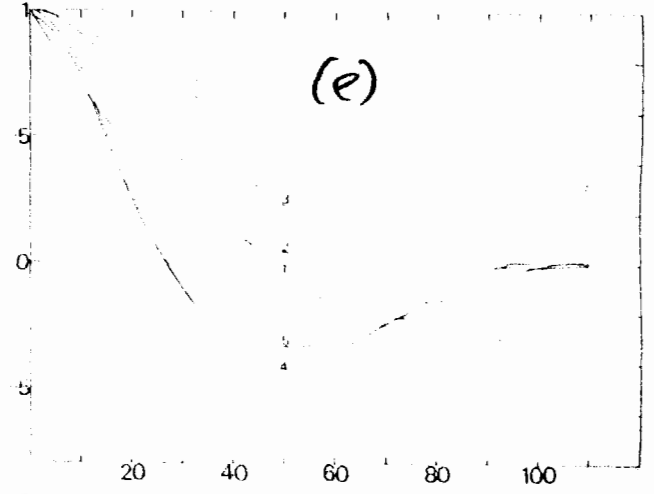
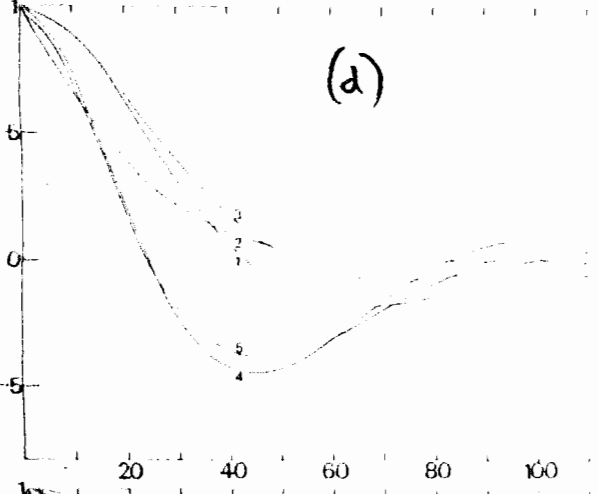
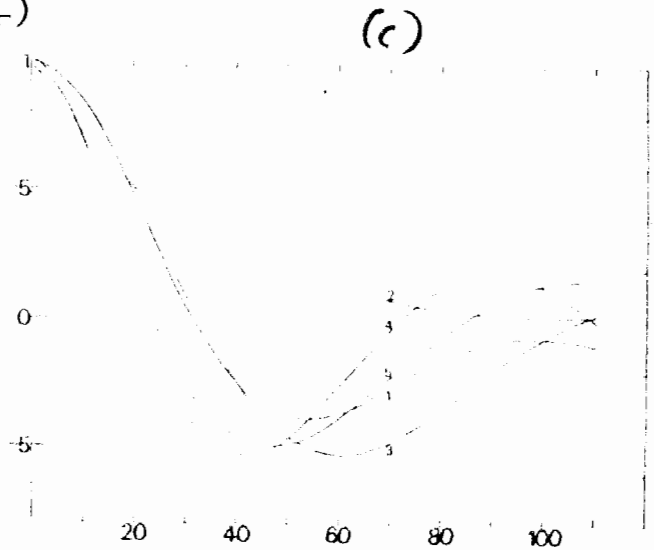
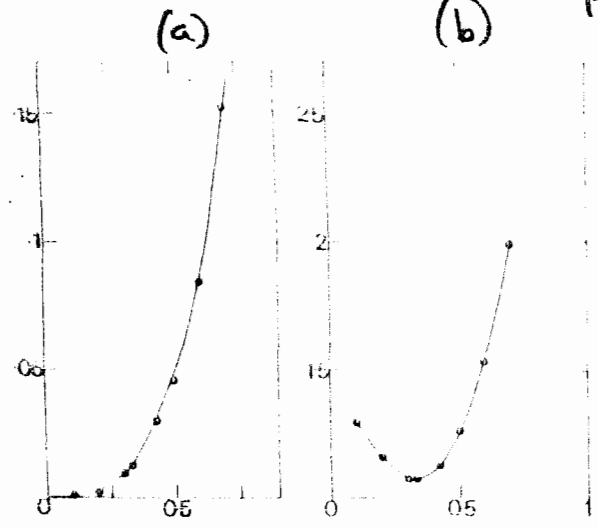
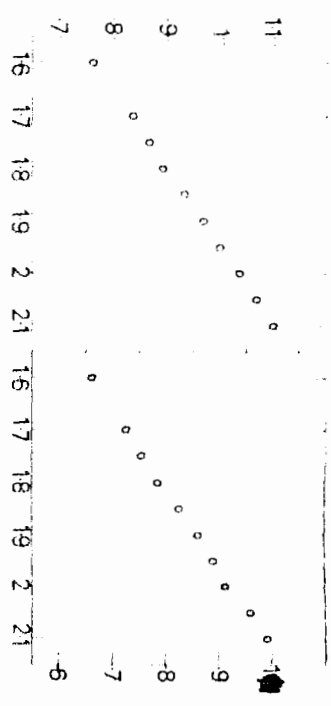
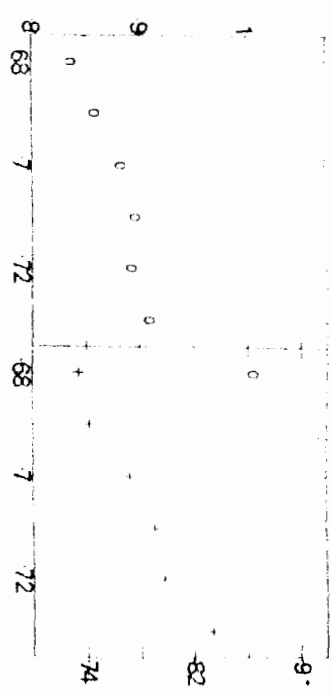


Fig (5)

(a)



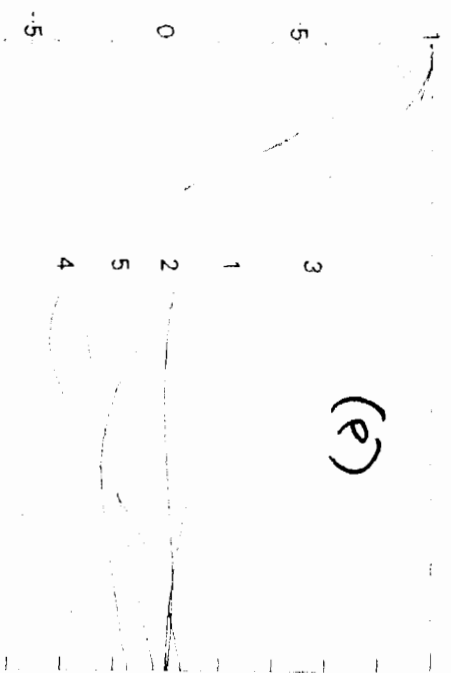
(b)



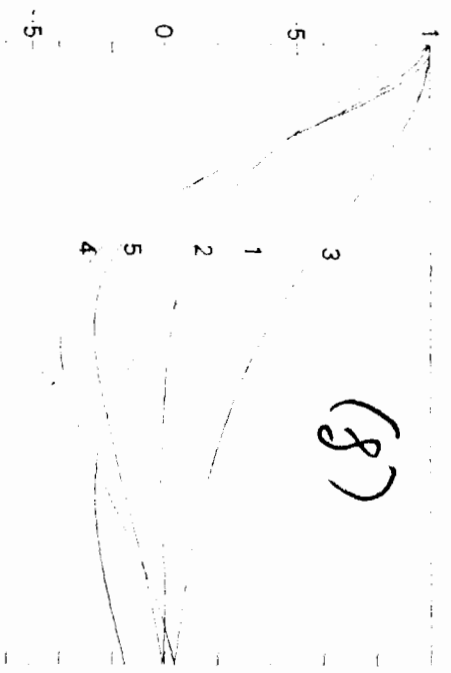
(c)

(d)

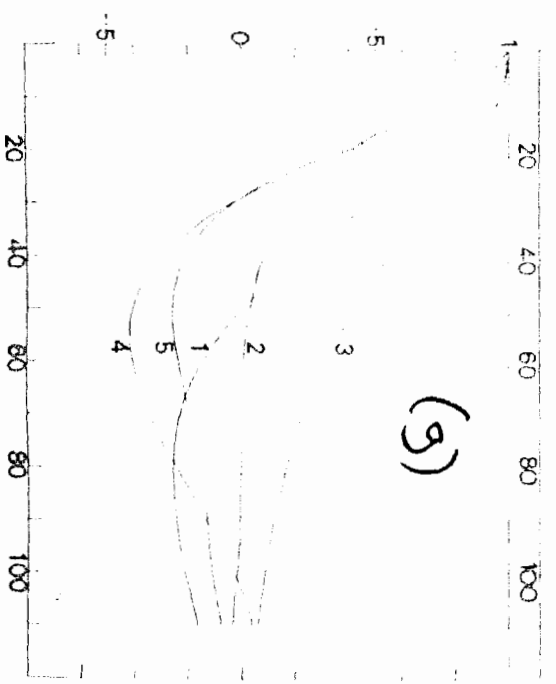
(e)



(f)



(g)



(h)

